






Exergy Analysis of a Solar Heating System in Indoor Spaces

Israa Ali Abdulghafor¹, Sinan A. Ali², Saif Ali Kadhim³, Hussein M. Al-Mrayatee¹, Karrar A. Hammoodi^{4*}

¹ Institute of Technology-Baghdad, Middle Technical University, Baghdad 10066, Iraq

² Control and Systems Engineering Department, University of Technology- Iraq, Baghdad 10066, Iraq

³ Mechanical Engineering Department, University of Technology- Iraq, Baghdad 10066, Iraq

⁴ Air Conditioning and Refrigeration Department, College of Technical Engineering, Warith Al- Anbiyaa University College, Karbala 56001, Iraq

Corresponding Author Email: karrar.al@uowa.edu.iq

Copyright: ©2024 The authors. This article is published by IETA and is licensed under the CC BY 4.0 license (<http://creativecommons.org/licenses/by/4.0/>).

<https://doi.org/10.18280/ijht.420508>

ABSTRACT

Received: 8 June 2024

Revised: 6 August 2024

Accepted: 21 August 2024

Available online: 31 October 2024

Keywords:

solar heating system, solar collector, radiator, indoor space, exergy analysis, exergy destruction

Energy consumption is rising in unison with population increase, industrialization, and urbanization. A solar heating system is one of the devices that supply consumers with thermal energy. Consequently, it is imperative to conduct an exergy analysis on this system in order to identify genuine, beneficial energy loss, which is not detectable by the first law of thermodynamics. The exergy analysis in this study is conducted using experimental data from the solar heating system in a space that includes a solar collector, pump, connections, and radiator, all of which operate with water as the working fluid. The exergy analysis is conducted for indoor heating spaces, radiators, and solar collectors under a variety of operating conditions, including a range of ambient temperatures and heating demands. The findings indicated that the rate of energy degradation is directly influenced by the heating burden and ambient temperature. The energy degradation rate in the solar collector increased by 14.25% when the ambient temperature varied from 15 to 21°C, while it decreased in the radiator and interior space by 55.59% and 57.57%, respectively. Conversely, as the heating capacity increased from 1100 to 1250 W, the energy degradation rate in the radiator and the indoor space increased by 15.45% and 19.81%, respectively.

1. INTRODUCTION

The type of room heating system you choose affects how much energy you use, how comfortable your home is, and how it affects the world [1, 2]. Energy analysis is important for system determination, but it is insufficient because it cannot quantitatively clarify the effects of working temperature levels. Exergy analysis can be used to quantify the efficiency of system operation and the amount of energy wasted [3, 4]. Exergy studies incorporate both the first and second laws of thermodynamics, while energy analysis just considers the first law [5-7]. In the engineering system which includes heating, cooling, ventilation systems and environment, the exergy has a wide application range [8-10]. Exergy analysis has gained significant popularity in several thermal applications, such as thermal power plants [11, 12], vapor compression refrigeration cycles [13, 14], organic Rankine cycles [15, 16], solar photovoltaic cells [17, 18], solar stills [19, 20], and solar cookers [21, 22]. Research on the use of exergy analysis in determining and controlling HVAC systems in buildings has just recently begun [23, 24]. In the most recent publication by Gonçalves et al. [25], the authors conducted research on the energy and exergy analysis of eight different space heating systems in various climates. Zhou and Gong [26] analyzed buildings energy systems in terms of the complete energy flow cycle. Suzuki [27] described the general framework of the

exergy balancing analysis. Furthermore, Suzuki offered the specific relationships required to calculate the energy equations of solar collectors. Luminosu and Fara [28] investigated the optimal operating mode of a flat solar collector by numerical simulations.

As prior studies have shown, and as far as the authors are aware, there has never been an exergy analysis for the entire heating system; thus, this study provides a comprehensive analysis of the exergy performance of the solar heating system under various operating situations. After the introduction, the study is organized into four sections: methodology, exergy analysis, findings and discussion, and conclusions.

2. METHODOLOGY

2.1 Materials and design

Although some studies discussed the related materials, the details of the solar heating system are unspecified [29]. This system has an interior room space of 2:5 meters in width, length, and height respectively. Figure 1 also indicates the installation of a flat-plate solar water heater on the outside surface of the building referring to the building roof, while the radiator for air heating is inside the building space. Each plate consists of 30 micro-channels linking two manifolds, a

chamber for water movement within the solar heat collection system, and the valves for water flow prior to the flat solar water heater. In the flat-plate solar water heater, hot water circulates in two headers and risers, where the intake header sends it through the riser, and the exit header, which takes water from the risers, passes it through plastic pipes to the radiator. In addition, to reduce the heat losses from the collection to the surrounding environment, thermal insulation is placed at the back and sides of the collector. Wrapped around the pipe plastic in the heating system is an aluminum casing that has a thickness of 2 mm The parameters of the flat plate solar collector shown in Table 1.

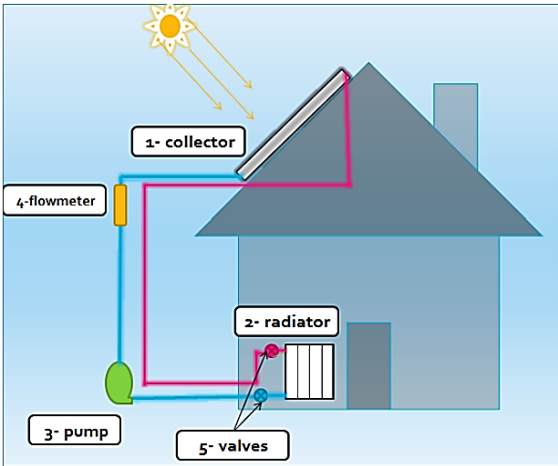


Figure 1. Solar heating system schematic diagram [29]

Table 1. The dimension specification of flat plate solar collector

Dimension Specification	Flat Plate Solar Collector
Dimension of collector	(2000×1000×80) mm
Glass cover thickness	3.2 mm
Transmittance of glass	95%
Aluminum Absorber plate thickness	0.4 mm
Absorber plate absorptivity	95%
Absorber emissivity	5%
Copper header tube diameter	22 mm / 2 headers
Copper riser tube diameter	8 mm / 7 risers
Space between riser tube	110 mm
Fiber glass insulation thickness	30 mm
Fiber glass density	60 kg/m ³
Air gap spacing between glass and absorber	25 mm

2.2 Theoretical basis and design rationale

The guidelines for the design of the experiment are enriched by the knowledge of the principles of thermodynamics and heat transfer. The choice regarding the material, size, and arrangement of components that are employed in the solar heating system depends on the aspects of thermal performance and heat losses. The design of the flat plate solar water heater entails solar energy collection whereby the flat plate collector has a relatively large surface area that is used in capturing solar energy. Thus, application of the risers and headers helps attain good distributions of water and proper heat transfer.

As for the choice of the insulating materials, and the aluminum casing, is to reduce thermal losses and accordingly the increase in the system’s efficiency. The sub-passages and

manifolds in the design of the radiator aim at improving convection between the hot water and room air for efficient heating of the premises. Due to the need of constant and reliable water supply in the cooling process, the pump and valve system is incorporated in the frame.

Incorporation of these theoretical considerations in the procedural design helps to achieve the maximum level of efficiency of the solar heating system, which forms the solid ground for the experimental procedures and data collection. This approach corresponds to existing literature at the same time as including a reputable theoretical framework to the experimental approach [29].

2.3 Study data

For the evaluation of the exergy of the solar heating system in the quasi-steady-state mode, the historical experimental data obtained in the study of Obaid [29] are used. The experiment was conducted on four separate days: January 9, January 20, February 20 and February 24 in the year 2019. The irradiance of the sun, wind and air temperatures in the environment were taken intermittently using portable instruments and a weather station from 9:00 a.m. to 5:00 p.m.,. The metallic absorbing plate exhibited a high level of absorbcency, efficiently converting solar irradiance into heat upon reaching the flat solar collector via the glass cover. Consequently, the absorber plate became heated, and the heat is transmitted from the absorber plate to the water by convection [30]. The pump sent the heated water from the collection to the radiator. The upper manifold tube is segmented into several smaller channels, via which the hot water is sent into the radiator. Convection facilitated the transport of heat from the hot water to the outside surface of the radiator. Subsequently, the hot water, excluding the lower manifold tube, was collected prior to being circulated back into the radiator. Finally, there is heat transfer by free convection and radiation between the surface of the radiator and the room. Throughout this procedure, the ambient temperature progressively rises until it reaches the designated internal temperature or just below.

3. EXERGY ANALYSIS

The second law of thermodynamics is used in energy optimization and the tool known as the Exergy analysis helps in this process. The quantity of power produced by a system that has an important function in determining the thermodynamics is the exergy. The energy analysis which follows the calculation of the solar heating system is shown in the Figure 2. Certain assumptions are made in order to enable analysis [31, 32]:

- (1) Each component is in a steady state and is flowing steadily.
- (2) The exergy destruction of the pump and valves are negligible.
- (3) Heat and pressure losses in the connecting pipes are negligible.
- (4) There is no heat exchange with the outdoor space.

The exergy balance for solar collector can be shown in Eq. (1) [33, 34]:

$$EX_{in} - EX_{out} - EX_d = 0 \tag{1}$$

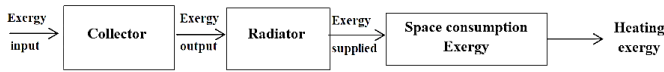


Figure 2. The exergy analysis

The total exergy rate that enters a solar collector may be determined by comparing the intake exergy rate with mass flow and the inlet exergy rate with solar irradiance absorbed by the collector, as shown in Eq. (2) [35].

$$EX_{in} = EX_{in,f} + EX_{in,q} \quad (2)$$

Inlet exergy rate with mass flow as follows in Eq. (3) [36]:

$$EX_{in,f} = m \cdot C_p (T_{w,in} - T_a - T_a \ln \frac{T_{w,in}}{T_a}) \quad (3)$$

Inlet exergy rate with solar irradiance absorbed by the collector as follows in Eq. (4) [33]:

$$EX_{in,q} = \eta_o G_t A_p (1 - \frac{T_a}{T_s}) \quad (4)$$

The apparent solar temperature represents by $T_s=6000$ K [37], optical efficiency represents by η_o and calculated from Eq. (5) [38]:

$$\eta_o = \frac{S}{G_t} \quad (5)$$

where, S is solar energy absorbed can be calculated using Eq. (6) [38]:

$$S = \frac{m \cdot C_p (T_{w,out} - T_{w,in})}{A_p} + U_1 (T_p - T_a) \quad (6)$$

where, U_1 overall heat loss coefficient can be found from [39, 40]:

$$U_1 = U_t + U_b + U_e \quad (7)$$

$$U_t = \left[\frac{N}{\left(\frac{c}{T_p} \right) \left(\frac{T_p - T_a}{N + z} \right)^e + \frac{1}{h_w}} \right]^{-1} + \left[\frac{\sigma (T_p + T_a) (T_p^2 + T_a^2)}{[\varepsilon_p + 0.00591 N h_w]^{-1} + \left[\frac{2N + z - 1 - 0.133 \varepsilon_p}{\varepsilon_g} \right] - N} \right] \quad (8)$$

$$z = (1 + 0.089 h_w - 0.1166 h_w \varepsilon_p) (1 + 0.07866 N) \quad (9)$$

$$c = 520 (1 - 0.00005 \beta^2) \text{ for } 0^\circ < \beta < 90^\circ \quad (10)$$

$$e = 0.43 \left(1 - \frac{100}{T_p} \right) \quad (11)$$

$$h_w = 2.8 + 3V \quad (12)$$

$$U_b = \frac{K_b}{X_b} \quad (13)$$

$$U_e = \frac{(L + W) H K_e}{L W X_e} \quad (14)$$

The outlet exergy rate represents by the outlet exergy rate with mass flow only and as the follows Eq. (15) [36]:

$$EX_{out} = EX_{out,f} = m \cdot C_p (T_{w,out} - T_a - T_a \ln \frac{T_{w,out}}{T_a}) \quad (15)$$

By three items, the exergy destruction rate can be represented and as follows Eq. (16) [41]:

$$EX_d = EX_{d,\Delta p} + EX_{d,\Delta T} + EX_{d,\Delta pf} \quad (16)$$

Exergy destruction rate produced by pressure declined through the tube as in Eqs. (17) and (18) [42]:

$$EX_{d,\Delta p} = \frac{m \cdot C_p}{\rho} \left(\frac{T_a \ln \frac{T_{w,out}}{T_a}}{T_{w,out} - T_{w,in}} \right) \quad (17)$$

$$\Delta P = \rho g (L_r \sin \beta + h_1) \quad (18)$$

The gravity acceleration represents by g , tube length represents by L_r , total pressure drop represent by h_1 and equal to Eq. (19) [42]:

$$h_1 = \frac{8m^2}{n_r g \rho^2 \pi^2 D_i^4} \left(f \frac{L_r}{D_i} + \sum_{i=1}^{n_r} K_L \right) \quad (19)$$

where, the number of tubes represent by n_r , partial pressure drops coefficient of connections represented by K_L which in tube's inlet equal to 1 and at outlet equal to 0.5, the friction coefficient represents by f and can be determined by Eq. (20a) and Eq. (20b) [43, 44]:

$$f = \frac{64}{Re} \text{ (Laminar flow)} \quad (20a)$$

$$f = \frac{64}{Re^{0.25}} \text{ (Turbulent flow)} \quad (20b)$$

Exergy destruction rate produced by the difference in the solar temperature with absorber plate surface can be shown in Eq. (21) [43]:

$$EX_{d,\Delta T} = \eta_o G_t A_p T_a \left(\frac{1}{T_p} - \frac{1}{T_s} \right) \quad (21)$$

Exergy destruction produced rate by the difference in temperature between absorber plate surface and working fluid can be shown in Eq. (22) [35]:

$$EX_{d,\Delta pf} = m \cdot C_p T_a \left(\ln \frac{T_{w,out}}{T_{w,in}} - \frac{T_{w,out} - T_{w,in}}{T_p} \right) \quad (22)$$

The exergy balance for radiator can be seen in Eq. (23a) and Eq. (23b) [45]:

$$\Delta EX_w - EX_{r,d} = EX_{r,out} \quad (23a)$$

$$\Delta EX_w = EX_{w,supply} - EX_{w,return} \quad (23b)$$

where, ΔEX_w represents the difference between the supply and return water exergy rate. The exergy rate of the supply water to the radiator and return water from radiator can be represented by $EX_{w,supply}$ and $EX_{w,return}$ respectively. $EX_{r,d}$ is the exergy destruction rate within radiator, and $EX_{r,out}$ is the exergy received by indoor from radiator.

The exergy rate supply and return water flows are determined by Eqs. (24a) and (24b) [25]:

$$EX_{w,supply} = m \cdot C_p \left((T_{w,out} - T_a) - T_a \ln \frac{T_{w,out}}{T_a} \right) \quad (24a)$$

$$EX_{w,return} = m \cdot C_p \left((T_{w,in} - T_a) - T_a \ln \frac{T_{w,in}}{T_a} \right) \quad (24b)$$

The exergy rate supplied to the indoor space from radiator can be seen in Eq. (25) [45]:

$$EX_{r,out} = Q_{heating} \left(1 - \frac{T_a}{T_{m,rs}} \right) \quad (25)$$

The exergy destruction rate in an interior area is calculated as the modification between the exergy rate provided to the indoor space and the rate at which exergy is lost due to heating.

$$EX_{sp,d} = EX_{r,out} - EX_{heating} \quad (26)$$

The heating exergy load rate expressed in Eq. (27) [46]:

$$EX_{heating} = Q_{heating} \left(1 - \frac{T_a}{T_i} \right) \quad (27)$$

4. RESULTS AND DISCUSSION

An examination is conducted on the effect of solar energy on the temperature of the water discharged from the solar collector in order to efficiently assess the performance of the system. According to Figure 3, there is a direct correlation between the increase in solar energy and the corresponding rise in water temperature from the solar collection. This happens no matter what temperature the water is coming in at. When the insolation was 750 W/m² and 100 W/m², the output water temperature increased by 5.30 percent and 9.12 percent, respectively, compared to an insolation of 500 W/m². Note that choosing a shadow-free site and determining the optimal azimuth and tilt angles can lead to the optimal orientation of solar collectors [47-50]. This will enable the collectors to collect the maximum amount of solar irradiance.

Figure 4 shows a study of the solar collector's exergy in relation to the temperature of the surrounding area. When the temperature outside goes up, both the rate at which energy is made by the water moving into the solar collector and the amount of sunlight that the collection plate absorbs go down. It seems that when the temperature of the surroundings goes up, heat is lost in both the water and the absorber plate because the process is irreversible.

The system's exergy rate largely determines the behavior of the outlet exergy rate with the ambient temperature, which remains consistent with the previous description. Due to

entropy creation in the solar collector, also known as irreversibility, the intake and output exergy rates differ. The rate of exergy destruction, also known as irreversibility, will undoubtedly grow with the rise in the temperature of the surrounding environment, as evidenced by the fact that it rose by 14.25% when the temperature of the surrounding environment went from 15 to 21 degrees Celsius. Energy producers exhibited this behavior in earlier investigations linked to this topic [51, 52].

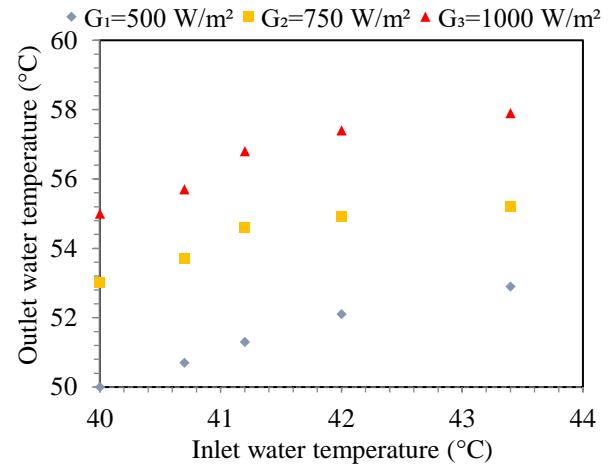


Figure 3. Influence of solar irradiance on water temperatures

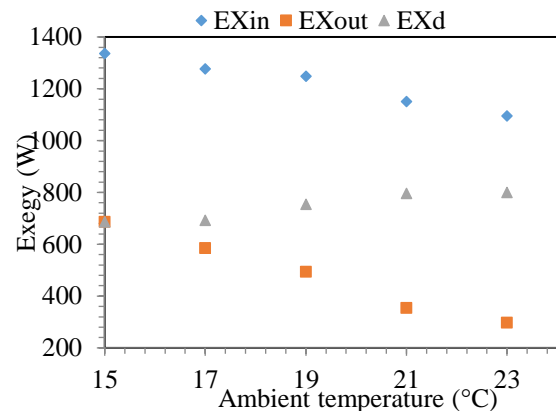


Figure 4. Influence ambient temperature on exergy rate in the solar collector

Figure 5 illustrates the exergy analysis of the radiator in relation to the surrounding environment's temperature. The radiator inputs an exergy rate equal to the observed exergy rate between the supply water and the return water. When the temperature of the surrounding environment rises, it is noticed that the input exergy rate falls. This decrease results in a drop in both the outlet energy rate from the radiator and the amount of energy supplied to the area. On the other hand, the change in ambient temperature from 15 to 21°C resulted in a 55.59% reduction in the energy destruction rate. This indicates that the rate of energy destruction decreases as the ambient temperature rises. This is due to the irreversibility of the entrance exergy rate, which leads to a greater amount of degradation than the outlet exergy rate. This behavior has been reported in applications that are comparable to exothermic radiators [52, 53].

Since the same exergy rate is received and delivered in the interior area, it is logical to expect a decrease in its value as the

temperature of the surrounding environment increases, as shown in Figure 6. However, as the ambient temperature increases, the rate of energy destruction in the interior area is reduced. This is rather logical because the energy requirements will be lower due to the reduction of the temperature difference necessary for the system and the temperature of the environment. With the change of the external environment temperature from 15 to 21°C the rate of energy dissipation in the interior area was reduced by 57%.

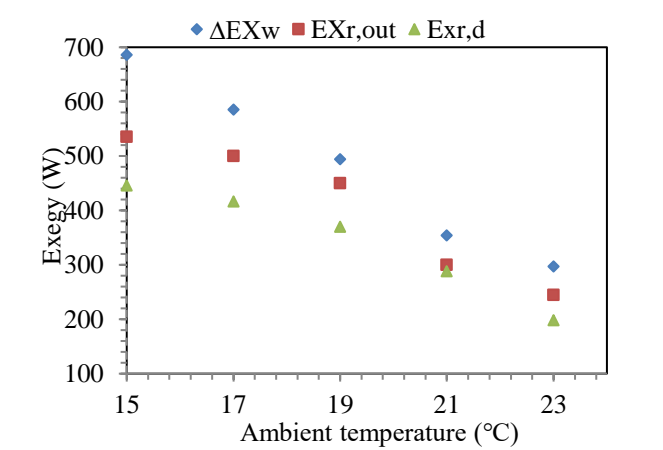


Figure 5. Influence ambient temperature on exergy rate in the radiator

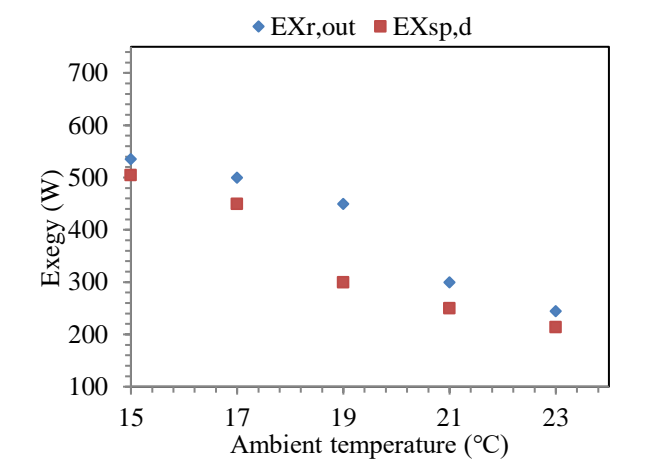


Figure 6. Influence ambient temperature on exergy rate in the indoor space

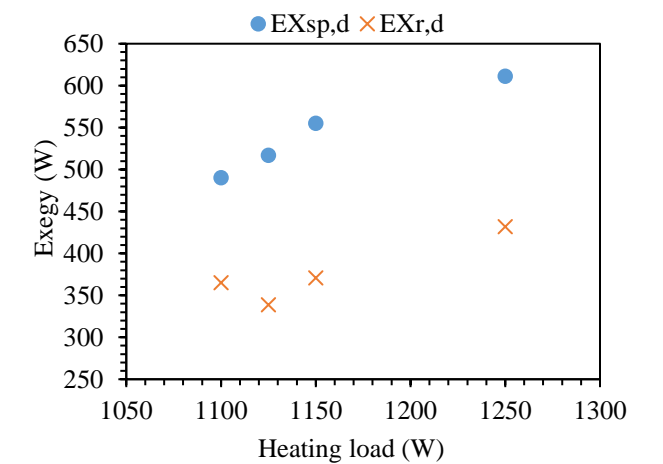


Figure 7. The exergy destruction rate at various heating load

Figure 7 illustrates the rate of exergy destruction in the radiator as well as the interior area, which is dependent on the amount of heating load. As the heating load increases, the rates of energy degradation rise, but in a nonlinear fashion. An increase in the heating load leads to an increase in entropy creation, subsequently causing a decrease in the exergy rate. To put that into perspective, the rate of energy degradation has a greater impact on the inside area than it does on the radiator. The exergy destruction rate of the radiator and the interior area increases by 19.81% and 15.45%, respectively, when the heating load increases from 1100 to 1250 W. This is the typical trend.

5. CONCLUSIONS

This study describes an energy analysis of a solar heating system, including a solar collector, radiator, and interior area that utilizes water as a working fluid. The analysis used data from experimental testing on a comparable system. The key discoveries of this investigation may be succinctly described as follows:

- The While the sun collector's exergy breakdown rate went up as the temperature outside went up, the rates at which it took in and released exergy went down.
 - As ambient temperature increased, the radiator's intake and output exergy rates decreased, as did its exergy destruction rate. Furthermore, increased heating demand led to a comparable increase in energy degradation.
 - As the temperature increased, energy destruction in the inner region reduced. However, the increase in heating demand led to a comparable increase in the rate of energy degradation.
 - The architecture and positioning angles of the solar collector system significantly influence its efficiency. This design feature effectively minimizes thermal losses and maximizes heat gains from sun irradiation.
 - The study suggests that as the ambient temperature increases, the energy destruction in the indoor space decreases. By regulating the thermal conditions of the building space and the ventilation to reduce the existing thermal gradient between the two spaces, we can improve the system's efficiency.
- This study offers useful insights into the quantitative and qualitative thermal efficiency of the solar heating system. This research may be expanded by investigating the decrease in energy destruction in the system through component replacement while also examining the economic viability of implementing such changes in the system.

REFERENCES

[1] Shukuya, M. (1994). Energy, entropy, exergy and space heating systems. In Healthy Buildings' 94, Proceedings of the 3rd International Conference, pp. 369-374.

[2] Hammoodi, K.A., Dhahad, H.A., Alawee, W.H., Omara, Z.M. (2024). Energy and exergy analysis of pyramid-type solar still coupled with magnetic and electrical effects by using Matlab simulation. *Frontiers in Heat and Mass Transfer*, 22(1): 217-262. <https://doi.org/10.32604/fhmt.2024.047329>

[3] Dovjak, M., Shukuya, M., Olesen, B.W., Krainer, A. (2010). Analysis on exergy consumption patterns for space heating in Slovenian buildings. *Energy Policy*,

- 38(6): 2998-3007. <https://doi.org/10.1016/j.enpol.2010.01.039>
- [4] Castellanos, H.G., Aryanfar, Y., Hammoodi, K.A., Ghriss, O., Keçebaş, A., Bouabidi, A., Ahmad, S., Ragab, A.E. (2024). Evaluation of the energy and exergy of a trans-critical CO₂ cycle driven by a double flash geothermal power plant. *Environmental Progress & Sustainable Energy*, 43(4): e14370. <https://doi.org/10.1002/ep.14370>
- [5] Choi, W., Ooka, R., Shukuya, M. (2018). Exergy analysis for unsteady-state heat conduction. *International Journal of Heat and Mass Transfer*, 116: 1124-1142. <https://doi.org/10.1016/j.ijheatmasstransfer.2017.09.057>
- [6] Sun, C., Fares, M.N., Sajadi, S.M., Li, Z., Jasim, D.J., Hammoodi, K.A., Nasajpour-Esfahani, N., Salahshour, S., Alizadeh, A.A. (2024). Numerical examination of exergy performance of a hybrid solar system equipped with a sheet-and-sinusoidal tube collector: Developing a predictive function using artificial neural network. *Case Studies in Thermal Engineering*, 53: 103828. <https://doi.org/10.1016/j.csite.2023.103828>
- [7] Abdul-Ghafoor, Q.J., Abed, S.H., Kadhim, S.A., Al-Maliki, M.A. (2024). Experimental and numerical study of a linear Fresnel solar collector attached with dual axis tracking system. *Results in Engineering*, 23: 102543. <https://doi.org/10.1016/j.rineng.2024.102543>
- [8] Shukuya, M. (2012). *Exergy: Theory and Applications in the Built Environment*. Springer Science & Business Media.
- [9] Abed, M.H., Al-Asadi, H.A., Oleiwi, A., Kadhim, S.A., Al-Yasiri, M., Alsayah, A.M., Nayyef, D.R. (2024). Improving building energy efficiency through ventilated hollow core slab systems. *Case Studies in Thermal Engineering*, 60: 104793. <https://doi.org/10.1016/j.csite.2024.104793>
- [10] Kadhim, S.A., Askar, A.H., Saleh, A.A.M. (2024). An enhancement of double pipe heat exchanger performance at a constant wall temperature using a nanofluid of iron oxide and refrigerant vapor. *Journal of Thermal Engineering*, 10(1): 78-87. <https://doi.org/10.18186/thermal.1429191>
- [11] Kaushik, S.C., Reddy, V.S., Tyagi, S.K. (2011). Energy and exergy analyses of thermal power plants: A review. *Renewable and Sustainable Energy Reviews*, 15(4): 1857-1872. <https://doi.org/10.1016/j.rser.2010.12.007>
- [12] Unal, F., Ozkan, D.B. (2018). Application of exergoeconomic analysis for power plants. *Thermal Science*, 22(6): 2653-2666. <https://doi.org/10.2298/TSCI170217098U>
- [13] Ali, H.M., Mahdi, L.A. (2023). Exergy analysis of chest freezer working with R-134a and R-600a at steady state conditions. *International Journal of Energy Production and Management*, 8(2): 63-70. <https://doi.org/10.18280/ijepm.080202>
- [14] Kadhim, S.A. (2024). Thermodynamic and environmental analysis of hydrocarbon refrigerants as alternatives to R134a in domestic refrigerator. *Journal of Thermodynamics*, 27(2): 1-9. <https://doi.org/10.5541/ijot.1368985>
- [15] Babaelahi, M., Sadri, S. (2022). Exergy cost accounting analysis of new hybrid solar organic Rankine cycle-MSF desalination system for Pasabandar region in Gwadar bay. *International Journal of Thermodynamics*, 25(3): 12-20. <https://doi.org/10.5541/ijot.1024316>
- [16] Malwe, P., Gawali, B., Shaikh, J., Deshpande, M., Dhalait, R., Kulkarni, S., Shindagi, V., Panchal, H., Sadasivuni, K.K. (2023). Exergy assessment of an organic rankine cycle for waste heat recovery from a refrigeration system: A review. *Chemical Engineering Communications*, 210(5): 837-865. <https://doi.org/10.1080/00986445.2021.1980396>
- [17] Prommas, R., Phiraphat, S., Rattanadecho, P. (2019). Energy and exergy analyses of PV roof solar collector. *International Journal of Heat & Technology*, 37(1): 303-312. <https://doi.org/10.18280/ijht.370136>
- [18] Kuczynski, W., Chliszcz, K. (2023). Energy and exergy analysis of photovoltaic panels in northern Poland. *Renewable and Sustainable Energy Reviews*, 174: 113138. <https://doi.org/10.1016/j.rser.2022.113138>
- [19] Hammoodi, K.A., Abed Dhahad, H., Alawee, W.H., Ibrahim Amro, M., Omara, Z.M., Essa, F.A. (2023). Experimental study on pyramid solar distiller performance with applying magnet field under various operating conditions. *Energy Sources, Part A: Recovery, Utilization, and Environmental Effects*, 45(4): 11410-11423. <https://doi.org/10.1080/15567036.2023.2258081>
- [20] Palaniappan, R., Murugesan, V., Govindasamy, K., Manirao, L. (2023). A comparative study on 3E (energy, exergy and economic) analysis of solar PV operated dome-shaped solar stills. *Thermal Science*, 27(5): 3805-3815. <https://doi.org/10.2298/TSCI220502168P>
- [21] Singh, O.K. (2021). Development of a solar cooking system suitable for indoor cooking and its exergy and enviroeconomic analyses. *Solar Energy*, 217: 223-234. <https://doi.org/10.1016/j.solener.2021.02.007>
- [22] Ibrahim, O.A.A.M., Kadhim, S.A., Ali, H.M. (2024). Enhancement the solar box cooker performance using steel fibers. *Heat Transfer*, 53(3): 1660-1684. <https://doi.org/10.1002/htj.23008>
- [23] Fan, B., Jin, X., Fang, X., Du, Z. (2014). The method of evaluating operation performance of HVAC system based on exergy analysis. *Energy and Buildings*, 77: 332-342. <https://doi.org/10.1016/j.enbuild.2014.03.059>
- [24] Omle, I., Askar, A. H., Kovács, E., Bolló, B. (2023). Comparison of the performance of new and traditional numerical methods for long-term simulations of heat transfer in walls with thermal bridges. *Energies*, 16(12): 4604. <https://doi.org/10.3390/en16124604>
- [25] Gonçalves, P., Gaspar, A.R., da Silva, M.G. (2013). Comparative energy and exergy performance of heating options in buildings under different climatic conditions. *Energy and Buildings*, 61: 288-297. <https://doi.org/10.1016/j.enbuild.2013.02.023>
- [26] Zhou, Y., Gong, G. (2013). Exergy analysis of the building heating and cooling system from the power plant to the building envelop with hourly variable reference state. *Energy and Buildings*, 56: 94-99. <https://doi.org/10.1016/j.enbuild.2012.09.041>
- [27] Suzuki, A. (1988). General theory of exergy-balance analysis and application to solar collectors. *Energy*, 13(2): 153-160. [https://doi.org/10.1016/0360-5442\(88\)90040-0](https://doi.org/10.1016/0360-5442(88)90040-0)
- [28] Luminosu, I., Fara, L. (2005). Determination of the optimal operation mode of a flat solar collector by exergetic analysis and numerical simulation. *Energy*, 30(5): 731-747. <https://doi.org/10.1016/j.energy.2004.04.061>

- [29] Obaid, M.J. (2020). Numerical and experimental study of solar water heater in heating a space. Thesis, Al-Furat Al-Awsat Technical University.
- [30] Shanmugan, S., Hammoodi, K. A., Eswarlal, T., Selvaraju, P., Bendoukha, S., Barhoumi, N., Mansour, M., Refaey, H.A., Rao, M.C., Mourad, A.I., Fujii, M., Elsheikh, A. (2024). A technical appraisal of solar photovoltaic-integrated single slope single basin solar still for simultaneous energy and water generation. *Case Studies in Thermal Engineering*, 54: 104032. <https://doi.org/10.1016/j.csite.2024.104032>
- [31] Askar, A.H., Kovács, E., Bolló, B. (2023). Prediction and optimization of thermal loads in buildings with different shapes by neural networks and recent finite difference methods. *Buildings*, 13(11): 2862. <https://doi.org/10.3390/buildings13112862>
- [32] Hammoodi, K.A., Mohsen, A.M., Omar, I., Al-Tajer, A. M., Basem, A. (2022). Using total equivalent temperature difference approach to estimate air conditioning cooling load in buildings. *International Journal of Current Engineering and Technology*, 12(3): 200-206.
- [33] Akpınar, E.K., Koçyiğit, F. (2010). Energy and exergy analysis of a new flat-plate solar air heater having different obstacles on absorber plates. *Applied Energy*, 87(11): 3438-3450. <https://doi.org/10.1016/j.apenergy.2010.05.017>
- [34] Ponnusamy, S., Gangadharan, S.S.K., Kalaiarasu, B. (2022). An exergy analysis for overall hidden losses of energy in solar water heater. *Thermal Science*, 26(1): 49-61. <https://doi.org/10.2298/TSCI200530343P>
- [35] Suzuki, A. (1988). A fundamental equation for exergy balance on solar collectors. *Journal of Solar Energy Engineering*, 110(2): 102-106. <https://doi.org/10.1115/1.3268238>
- [36] Farahat, S., Sarhaddi, F., Ajam, H. (2009). Exergetic optimization of flat plate solar collectors. *Renewable Energy*, 34(4): 1169-1174. <https://doi.org/10.1016/j.renene.2008.06.014>
- [37] Khafaji, H.Q., Abdul Wahhab, H.A., Al-Maliki, W.A.K., Alobaid, F., Epple, B. (2022). Energy and exergy analysis for single slope passive solar still with different water depth located in Baghdad center. *Applied Sciences*, 12(17): 8561. <https://doi.org/10.3390/app12178561>
- [38] Jafarkazemi, F., Ahmadifard, E. (2013). Energetic and exergetic evaluation of flat plate solar collectors. *Renewable Energy*, 56: 55-63. <https://doi.org/10.1016/j.renene.2012.10.031>
- [39] Duffie, J.A., Beckman, W.A., Blair, N. (2020). *Solar Engineering of Thermal Processes, Photovoltaics and Wind*. John Wiley & Sons.
- [40] Jasim, M.A. (2014). Utilization of air-water solar collector system for space heating. Theses, University of Technology- Iraq.
- [41] Kar, A.K. (1989). Exergy optimization of flow rates in flat-plate solar collectors. *International Journal of Energy Research*, 13(3): 317-326. <https://doi.org/10.1002/er.4440130308>
- [42] Cengel, Y., Cimbala, J., Turner, R. (2012). *EBOOK: Fundamentals of Thermal-Fluid Sciences (SI units)*. McGraw Hill.
- [43] Bussman, W., Baukal Jr, C.E. (2019). Fluid flow. *Industrial Combustion Testing*, 101-120.
- [44] Hammoodi, K.A., Hasan, H.A., Abed, M.H., Basem, A., Al-Tajer, A.M. (2022). Control of heat transfer in circular channels using oblique triangular ribs. *Results in Engineering*, 15: 100471. <https://doi.org/10.1016/j.rineng.2022.100471>
- [45] Kazanci, O.B., Shukuya, M., Olesen, B.W. (2016). Exergy performance of different space heating systems: A theoretical study. *Building and Environment*, 99: 119-129. <https://doi.org/10.1016/j.buildenv.2016.01.025>
- [46] Shukuya, M. (1994). Energy, entropy, exergy and space heating systems. *Mechanical Engineering*, 1: 369-374. https://www.researchgate.net/publication/281306405_Energy_entropy_exergy_and_space_heating_systems.
- [47] Al-Ghezi, M.K., Mahmoud, B.K., Alnasser, T., Chaichan, M.T. (2022). A comparative study of regression models and meteorological parameters to estimate the global solar radiation on a horizontal surface for Baghdad City, Iraq. *International Journal of Renewable Energy Development*, 11(1): 71-81. <https://doi.org/10.14710/ijred.2022.38493>
- [48] Kadhim, S.A., Al-Ghezi, M.K., Shehab, W.Y. (2023). Optimum orientation of non-tracking solar applications in Baghdad City. *International Journal of Heat and Technology*, 41(1): 125-134. <https://doi.org/10.18280/ijht.410113>
- [49] Ibrahim, O.A.A.M., Kadhim, S.A., Al-Ghezi, M.K.S. (2023). Photovoltaic panels cooling technologies: Comprehensive review. *Archives of Thermodynamics*, 44(4): 581-617. <https://doi.org/10.24425/ather.2023.149720>
- [50] Reda, S.M.A.M., Hussein, M.A.M., Hadi, J.M., Al-Asadi, H.A., Hammoodi, K.A., Ayed, S.K., Majdi, H.S. (2024). Optimizing tilt angle for thermal efficiency of vacuum tube solar collectors. *International Journal of Energy Production and Management*, 9(1): 57-64. <https://doi.org/10.18280/ijepm.090107>
- [51] Acir, A., Bilginsoy, A.K., Coşkun, H. (2012). Investigation of varying dead state temperatures on energy and exergy efficiencies in thermal power plant. *Journal of the Energy Institute*, 85(1): 14-21. <https://doi.org/10.1179/174396711X13116932752074>
- [52] Bilgili, M.E.H.M.E.T., Ozbek, A., Yasar, A., Simsek, E., Sahin, B. (2016). Effect of atmospheric temperature on exergy efficiency and destruction of a typical residential split air conditioning system. *International Journal of Exergy*, 20(1): 66-84. <https://doi.org/10.1504/IJEX.2016.076679>
- [53] Kopac, M., Hilalci, A. (2007). Effect of ambient temperature on the efficiency of the regenerative and reheat Çatalağzı power plant in Turkey. *Applied Thermal Engineering*, 27(8-9): 1377-1385. <https://doi.org/10.1016/j.applthermaleng.2006.10.029>

NOMENCLATURE

A	area, m ²
C _p	specific heat of water, J/kgK
c	coefficient to find top surface heat loss
D _i	inlet tube diameter, m
EX	exergy rate, W
e	coefficient to find top surface heat loss
f	friction coefficient
G _t	solar irradiance, W/m ²
g	gravity acceleration, m/s ²

H	collector thickness, m
h_w	wind heat transfer coefficient, W/m^2K
h_l	total pressure drop, Pa
K	insulation thermal conductivity, W/mK
K_L	pressure drop coefficient of connections
L	collector length, m
L_r	tube length, m
\dot{m}	mass flow rate of water, kg/s
N	number of covers
n_r	number of tubes
P	pressure, Pa
Q_{he}	heating load, W
Re	Reynolds number
S	solar energy absorbed, W/m^2
T	temperature, K
U	heat loss coefficient, W/m^2K
V	wind speed, m/s
W	collector width, m
X	insulation thickness, m
z	coefficient to find top surface heat loss

Greek symbols

Δ	different
β	tilt angle, deg
ε	emittance
π	Pi (3.1415)
σ	Stefan-Boltzmann constant, W/mk^4

η_o	optical efficiency
----------	--------------------

Subscripts

a	ambient
b	back
c	consumption
d	destruction
e	edge
f	flow
g	glass
i	operative
in	inlet
l	overall losses
m	mean
out	outlet
p	plate
q	solar irradiance
r	received by indoor from radiator
rs	radiator surface
s	solar
sp	space
t	top
w	water
ΔP	pressure declined through the tube
ΔP_f	difference between the water temperature and absorber plate temperature
ΔT	difference between the solar temperature and absorber plate temperature